

# Domain Size of Dynamic Heterogeneities Just above the Glass Transition in an Amorphous Polycarbonate

K.-L. Li, Alan Anthony Jones,\* and Paul T. Inglefield

Department of Chemistry, Clark University, Worcester, Massachusetts 01610

A. D. English†

Central Research and Development Department, Experimental Station, E. I. du Pont de Nemours and Company, Wilmington, Delaware 19898. Received January 5, 1989; Revised Manuscript Received March 28, 1989

**ABSTRACT:** The proton NMR free induction decay and associated line shape show the presence of at least two components in a nominally amorphous polycarbonate 40–60 K above the glass transition. Since only phenylene protons are present in this polymer, the faster decaying component of the free induction decay is associated with less mobile regions and the slower decaying component is associated with more mobile regions. To characterize the size of these dynamic heterogeneities, a Goldman–Shen experiment was performed and spin diffusion from the more mobile domain to the less mobile domain was observed. The time scale for spin diffusion was 10–250 ms. These times are used to calculate the size of the more mobile domain by using an estimated value of the diffusion constant for spin diffusion. The best determination of the more mobile domain is 30 Å, though the technique is consistent with domain sizes ranging from 10 to 100 Å. The fraction of polymer in the more mobile domains is about 15% at the temperatures studied so the structural picture can be summarized as small islands of mobile material surrounded by larger regions of lesser mobility. As the temperature is increased, the fraction of mobile material appears to increase through growth in size of the more mobile islands. If the domain size is extrapolated to lower temperatures, the onset of mobility at the glass transition is associated with very small domains that are comparable to the repeat unit itself.

## Introduction

NMR spectroscopy has been quite successful in defining the character of local chain dynamics in bulk polymers. Proton,<sup>1</sup> fluorine,<sup>2</sup> carbon,<sup>3</sup> and deuterium<sup>4–6</sup> nuclei have all been exploited in this endeavor, with the latter two nuclei being most informative over the last decade or so. One of the important features of the studies of dynamics in glassy systems has been the determination of the inhomogeneity of local dynamics.<sup>3–6</sup> Both below and near the glass transition in nominally amorphous polymers, local motions are found to be heterogeneous in that the same chemical moiety in different spatial locations within a single glassy sample may have different rates and geometries of motion. In proton spectroscopy, this has been discussed in terms of more mobile and less mobile components of amorphous material making distinguishable contributions to the line shapes just above the glass transition.<sup>7–12</sup> Below the glass transition, carbon-13 relaxation times in the rotating frame also reflect the heterogeneous character of the glass.<sup>3</sup> Perhaps deuterium line shapes in glassy polymers are the clearest manifestation of the variety of mobilities present in a given glassy sample.<sup>4,5</sup>

The question pursued in this work is the spatial size of the dynamic heterogeneities in an amorphous system at a temperature just above the glass transition. Since the material is chemically homogeneous at the level of the repeat unit and is nominally single phase, few experimental techniques would appear to be applicable. If the heterogeneities may be described as discreet domains of either differing density or local conformation, it may be possible to characterize them with scattering methods. In either case, density differences are a distinct possibility, but identification of these particular density fluctuations with scattering methods is at best difficult.

Since NMR spectroscopy was the method first used to identify spatial heterogeneity of local motions, it is natural to use this method to characterize the properties of these domains. The domains are believed to be too small to be

characterized by magnetic resonance imaging at its current state of development, though this approach is at least a conceptual possibility. One NMR experiment, the Goldman–Shen (GS) experiment,<sup>13</sup> has been used to study spatial properties on the basis of differences in mobility. This experiment has been applied to polymer systems, including the pioneering work of Assink on hard and soft regions in polyurethanes,<sup>14–16</sup> and by other investigators on crystalline and noncrystalline regions in semicrystalline polymers.<sup>17–21</sup> The technique has not been widely utilized, because scattering and diffraction techniques are usually superior. However, for the system of interest here, the GS experiment seems to be the best choice since the ability to differentiate spatial regions on the basis of their differences in  $T_2$  (mobility) has been established.<sup>12</sup>

There are a number of possible variations of the classic GS experiment that could be applied,<sup>17,20,21</sup> but the original version is employed in this study. In this version, the spin-lattice relaxation times ( $T_1$ ) of each component are assumed to be much longer than the duration of the entire GS experiment. Transverse magnetization is created by a simple  $\pi/2$  pulse as shown in Figure 1. A delay time,  $t_0$ , is selected during which the magnetization associated with less mobile regions is allowed to dephase. If the rate or amplitude of motion in the more mobile region is sufficiently large relative to that in the less mobile region, some of the magnetization of the more mobile region will still exist along the  $x$  axis in the rotating frame after the less mobile magnetization has dephased. In terms of relaxation times, the less mobile region has a short spin-spin relaxation time ( $T_{2l}$ ) and the more mobile regions has a longer spin-spin relaxation time ( $T_{2m}$ ). This difference in  $T_2$ 's is the physical property employed to discriminate between the two domains. In the next part of the experiment, spin diffusion among abundant spins is used to establish the domain size. A second  $\pi/2$  pulse of opposite phase to the first is applied to restore the magnetization associated with the more mobile component to the  $z$  axis. A variable mixing time,  $t$ , is allowed to pass before a third  $\pi/2$  pulse of the same phase as the first is applied. The third pulse places the magnetization back in the  $xy$  plane for observation. During the mixing time,  $t$ , spin diffusion

† Contribution No. 4999.

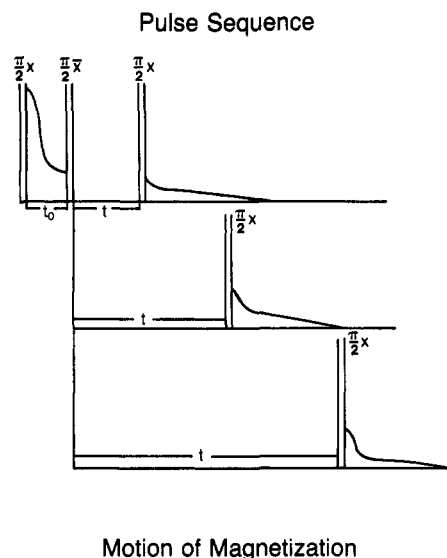


Figure 1. Goldman-Shen pulse sequence and the associated motion of the magnetization.

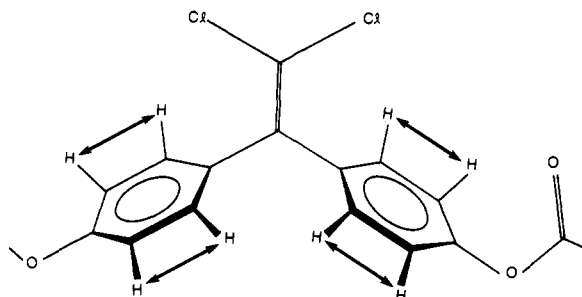


Figure 2. Polycarbonate repeat unit. The dominant intramolecular dipolar interaction is schematically indicated by the double-headed arrow.

will occur. This process will transfer magnetization from the more mobile domains to the less mobile domains. If the two domains have distinguishable line shapes or  $T_2$ 's the amount of transferred magnetization can be determined as a function of time  $t$ . The amount and rate of magnetization transfer can subsequently be used to calculate domain size if the diffusion constant for spin diffusion is known and a model geometry is assumed. There are uncertainties in the analysis of the data<sup>14-17</sup> (see below) but spatial properties in agreement with scattering methods have been previously determined with the GS experiment.<sup>15</sup>

The structure of the polymer selected for this study is shown in Figure 2 and has been the subject of several other studies below the glass transition<sup>22,23</sup> and one other study just above the glass transition.<sup>12</sup> This latter study, via a line-shape analysis, has determined the populations of the more and less mobile components. This polymer is convenient for proton NMR studies because it contains only a single type of proton and the predominant interaction determining the proton line shape is a dipolar coupling between adjacent phenylene protons. The vector between the adjacent protons is parallel to the virtual backbone bond, making this interaction and the associated observ-

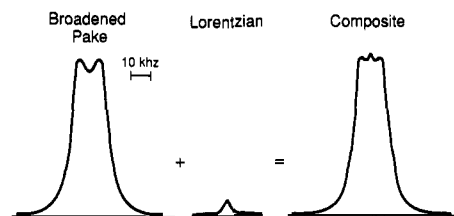


Figure 3. Line shapes for the two components used to simulate<sup>12</sup> the proton line shape at 181 °C.

ables good indicators of segmental motion. Figure 3 shows the two line-shape components used to simulate the line shape at 181 °C, which emphasizes the basis for considering the presence of two domains. The existence of two distinct domains characterized by high and low mobilities does not necessarily imply the absence of a broad range of mobilities being present in the amorphous polymer. The success of the GS experiment, however, does point to the existence of spatial entities characterized by differences in overall mobility. This point is addressed in some detail in the Discussion.

### Experimental Section

The polycarbonate shown in Figure 2 was supplied by General Electric Research and Development and is part of the same lot used in earlier studies.<sup>12,22,23</sup> The intrinsic viscosity is 0.5 dL/g. Typically, the sample is dried for 2 days under vacuum at 120 °C in a 10-mm NMR tube and then sealed. The glass transition temperature of the polycarbonate is 157 °C (DSC) and the temperature range of this study is around 200 °C, where the relative population of the more mobile and less mobile components fall in a convenient range as determined in the earlier line-shape investigation.<sup>12</sup> Near 200 °C the more mobile component constitutes about 15% of the total magnetization, which is comparable to population ranges considered in other GS experiments on polymers.<sup>14-17</sup>

Proton NMR spectra were acquired on a Bruker SXP NMR spectrometer at a Larmor frequency of 90 MHz. For  $\pi/2$  pulses, the pulse width was set at 2.5  $\mu$ s and dwell times of around 10  $\mu$ s were used, which corresponds to a quadrature sweep width of 100 kHz. Proton line widths were approximately 10 kHz in the temperature range under investigation. Temperature control was maintained to within 2 deg with a Bruker BST 100/700 temperature controller that was calibrated against a thermocouple in a sample tube in the probe.

The  $t_0$  pulse separation in the Goldman-Shen sequence varied from 150 to 300  $\mu$ s and was selected so that the magnetization of the less mobile component would have nearly completely decayed while a still appreciable amount of the more mobile magnetization persisted. The ratio of the more mobile to less mobile magnetization at the beginning of the mixing time varied from 5 to 200 depending upon temperature, and  $t_0$  values greater than 10 were deemed desirable.

The mixing time,  $t$ , was varied from 0.2 to 60 ms with the rate of repopulation of the less mobile magnetization dictating the choice of this variable. It is important that the mixing time be short with respect to  $T_1$  which was achieved since the  $T_1$ 's are of the order of seconds in the temperature range studied.

### Results

Three typical GS free induction decays (FID's) at a temperature of 202 °C are shown in Figure 4. The first FID (Figure 4A) is taken at a rather short mixing time and it may be characterized as a single exponential decay. This is to be expected since at short mixing times only the magnetization from the more mobile domain should be present. The second FID, Figure 4B, shows the behavior of the GS FID after a sufficient time, 1.5 ms, has elapsed so that the magnetization of the less mobile component has been somewhat repopulated by spin diffusion. The FID is now fairly obviously composed of more than one component and the situation is even more pronounced

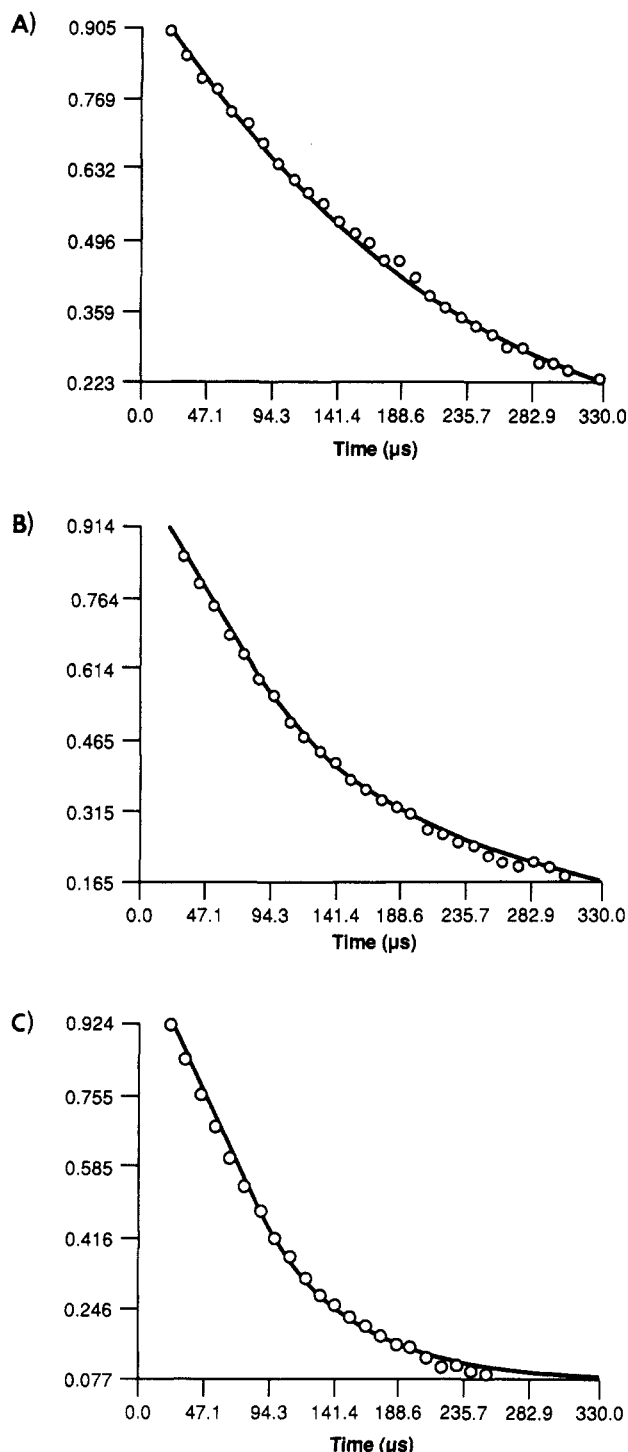


**Figure 4.** Goldman-Shen free induction decays: (A) for a mixing time of 200  $\mu$ s; (B) for a mixing time of 1.5 ms; (C) for a mixing time of 36 ms. The lines are fits of the free induction decays as described in the text.

after 36 ms as shown in Figure 4C. The selection of only the more mobile component at short values of  $t$  and the repopulation of the less mobile component at long values of  $t$  demonstrate the basic applicability of the GS experiment to this problem.

To quantitatively characterize the GS FID's, the treatment of Assink<sup>14-16</sup> will be followed. The less mobile component of the magnetization will be treated as Gaussian. Figure 5 shows the fit of this component of the line shape obtained in the earlier<sup>12</sup> study on the relative populations of the more mobile and less mobile components. This calculated line shape is a Gaussian broadened Pake pattern, but the broadening is so large that the Pake

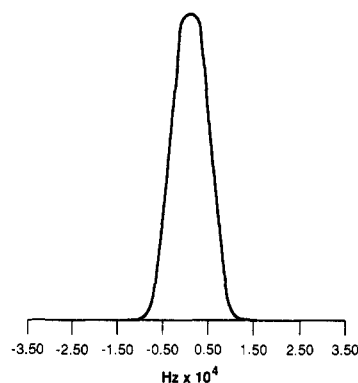


**Figure 5.** Less mobile line shape. This is part of the fit of the total line shape at 194 °C from an earlier line-shape study.<sup>12</sup>

**Table I**  
 **$T_2$ 's + Fractional Populations**

temp, °C	less mobile fraction	$T_{2m}$ , $\mu$ s		$T_{2l}$ , $\mu$ s	
		GS FID <sup>a</sup>	line shape	GS FID	line shape
194	0.892		138		59
197		150-180		65-80	
199			168		82
202		190-220		75-90	
204	0.850		227		103
207		290-330		90-115	
208	0.834		318		134

<sup>a</sup>  $T_2$ 's in the GS experiment depend on evolution time.<sup>14-16</sup>

splitting is obscured. Given this characteristic, the less mobile contribution to the FID will be treated as purely Gaussian with the standard form

$$G_1(t) = Ae^{-(t/T_{2l})^2} \quad (1)$$

In the line-shape study to establish the relative populations, the narrow component of the line was described by a Lorentzian line. For fitting the GS FID, the time domain form of the Lorentzian will be used.

$$G_m(t) = (1 - A)e^{-(t/T_{2m})} \quad (2)$$

The composite GS FID will then be fit to the form

$$G(t) = Ae^{-(t/T_{2l})^2} + (1 - A)e^{-(t/T_{2m})} \quad (3)$$

so that the quantity  $A$  can be used to monitor the repopulation of the less mobile component as a function of time. The  $T_2$ 's obtained by fitting the GS FID's and those obtained previously,<sup>12</sup> by fitting line shapes, are comparable. The  $T_2$ 's in the GS experiment are dependent on mixing time as was noted by Assink.<sup>14-16</sup> The fits are shown in Figure 4 and the  $T_2$  data are summarized in Table I.

The recovery of the less mobile component of the magnetization detected after the GS pulse sequence is monitored by the quantity  $R(t)$  where

$$R(t) = A(t)/A(\infty) \quad (4)$$

and  $A(\infty)$  is the population of the less mobile component at time infinity in the absence of spin lattice relaxation. The recovery plots are shown in Figures 6-8 as a function of the square root of the mixing time  $t$  as is traditional.<sup>17</sup>

**Interpretation.** Expressions for the recovery factor,  $R(t)$ , have been developed by Cheung and Gerstein in terms of the domain thickness,  $b$ , and the spin diffusion constant,  $D$ . These expressions apply to the case where spin lattice relaxation may be neglected, which is appropriate for the experimental situation under consideration. A second simplifying assumption is that the distribution of more mobile domains within the sample is described by

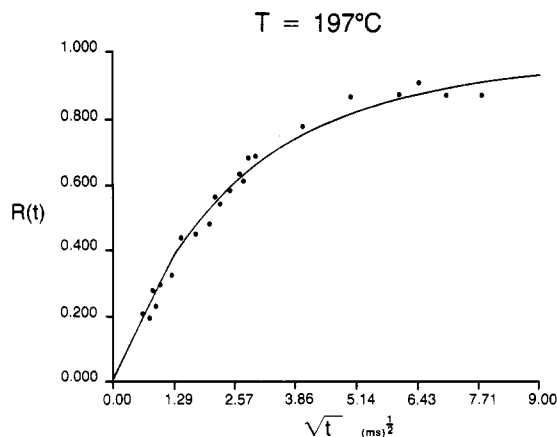


**Figure 6.** Recovery factor versus the square root of time at 197 °C. The line is a fit based on three-dimensional diffusion and allows for variation of the long-time limit.

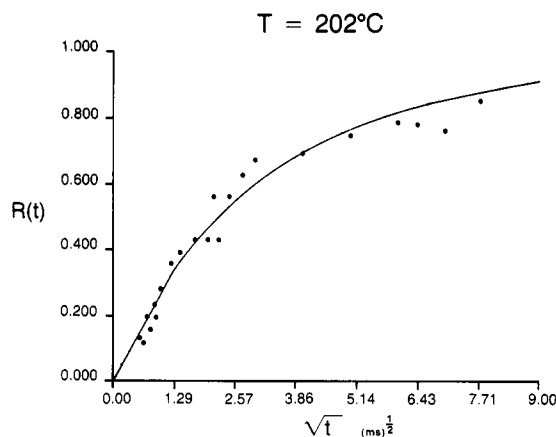


**Figure 7.** Recovery factor versus the square root of time at 202 °C. The line is a fit based on three-dimensional diffusion and allows for variation of the long-time limit.

a Poisson distribution for the random spacing ( $b$ ) of domains. This distribution for random spacing of the domains seems reasonable for the case at hand. The recovery factor for a one-dimensional system is given by

$$R(t) = 1 - \phi(t)$$

$$\phi(t) = \exp(Dt/b^2) \operatorname{erfc}(Dt/b^2)^{1/2} \quad (5)$$

Note that  $\phi(t)$  is the normalized autodiffusion function and is of a standard form for one-dimensional diffusion<sup>24</sup> and has been used in other contexts. The function  $\phi(t)$  has a value of 1 at time zero and a value of 0 at time infinity. The generalized autodiffusion function for three dimensions can be obtained by cubing the one-dimensional solution, which leads to the following expression for the recovery factor

$$R(t) = 1 - \phi_x(t)\phi_y(t)\phi_z(t) \quad (6)$$

where each of the  $\phi_i(t)$  has the form given in eq 5. Given the nature of the system under investigation, the three-dimensional form of the recovery equation will be employed. Different dimensionalities would be appropriate for either different spatial distributions of domains or if the diffusion constants were anisotropic. An example of the first case might be lamellar morphologies in semicrystalline polymers, but there are no such morphological characteristics in the system under study, which would point toward a lower dimensionality solution. The second factor that might lead to a choice of dimensionality other than three is anisotropic spin diffusion. A source of such behavior might be strong intramolecular dipolar interac-

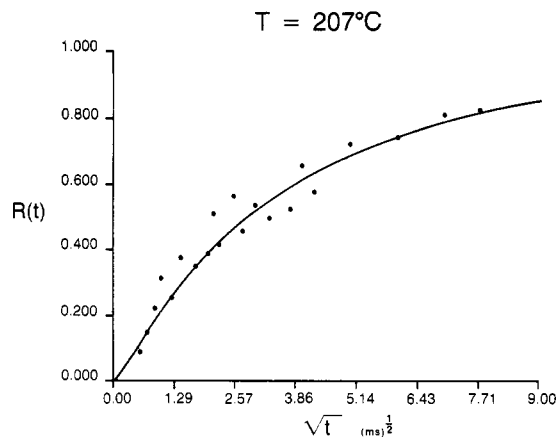


**Figure 8.** Recovery factor versus the square root of time at 207 °C. The line is a fit based on three-dimensional diffusion and allows for variation of the long-time limit.

tions such that spin diffusion along the chain direction would be preferred. Two factors oppose such possibilities in the polycarbonate chosen. First, the intramolecular and intermolecular contributions to the second moment of the proton line shape are equal.<sup>22</sup> Second, polycarbonate is a very flexible polymer so that the chain direction should not be preferential even from a fairly local view point.

One-, two-, and three-dimensional forms were used to fit the data and in terms of the quality of the fits there was little reason to select one dimensionality over another. The basic parameter of the fitting of the recovery factor expressions to the data of Figures 6–8 is  $D/b^2$ . The most straightforward consideration would indicate that the recovery factor should become one at long mixing times. A value of one corresponds to a relative population of less mobile to more mobile in accordance with that determined from the line-shape experiments.<sup>12</sup> In the fitting of magnetization recovery, if the long-time limit was allowed to deviate from one, slightly better fits were obtained with values near 0.90–0.95. This observation is similar to the findings of Cheung and Gerstein<sup>17</sup> who discussed some considerations that could lead to recovery factors slightly less than one in the long-time limit. In the fitting of  $R(t)$  reported here, the long-time limit will be allowed to deviate from one.

Employing eq 5 to analyze the magnetization recovery data requires some caution. The derivation<sup>17</sup> of this equation assumes that the spin diffusion constants are equal in both domains. It is clear that the spin diffusion constant, which relies upon static dipolar couplings, must be smaller in the more mobile domain. In the present case the  $T_2$ 's of the two domains differ only by a factor of 2–3, which indicates that the spin diffusion constants differ by less than a factor of 5. (Note that since the less mobile component is Lorentzian, there is a substantially larger difference in FID decay rates than there is in the  $T_2$ 's.) Other factors that could lead to greater differences in  $D$  such as significantly different densities, the anisotropy of crystalline regions, or different chemical repeat units in the two domains are not relevant here. However, the mixing time ( $t$ ) of the experiment, during which magnetization is allowed to diffuse, relative to  $b^2/D$  is of relevance. The mixing time of the experiment must vary over a range of much less than  $b^2/D$  up to a range of the order of  $b^2/D$  to effectively monitor spin diffusion in both domains. Therefore, at small values of  $t$  an analysis where  $D_m < D_l$  is explicitly included would be appropriate and at large values of  $t$  an analysis with  $D_m = D_l$  should be used. In the present case, this apparent dichotomy may be resolved by using the analysis that assumes equal spin

**Table II**  
 **$D/b^2$  from Recovery Factor Fits**

temp, °C	dimensionality of fit, (ms) <sup>-1</sup>			
	1D	2D	3D	3D(var lim)
197	0.14	0.030	0.010	0.014
202	0.08	0.016	0.0059	0.0095
207	0.052	0.010	0.0040	0.0061

**Table III**  
**Spin Diffusion Constants**

temp, °C	10 <sup>12</sup> $D$ , cm <sup>2</sup> /s	
	Assink	Cheung and Gerstein
197	1.71	1.16
202	1.37	0.90
207	0.91	0.71

diffusion constants in both domains and setting  $D = D_m$ ; this treatment is justified because at short mixing times the magnetization recovery equations<sup>17</sup> for both  $D_m \ll D_l$  and  $D_m = D_l$  have the same form and at longer mixing times the equal diffusion constant model is appropriate.

With the limitations of eq 5 just reviewed recognized, the fits of the experimental data are shown in Figures 6–8 for the three-dimensional form with an adjustable long-time limit. The associated parameters are reported in Table II along with some parameters of other fits to indicate the sensitivity of the results to the choice of the fitting form. To extract a domain size from the fits of the recovery factor, a value of the spin diffusion constant,  $D$ , must be determined. Several expressions have been presented to calculate  $D$  from the spin–spin relaxation time and intrinsic distances of the system. The earliest equation for  $D$  was presented by Assink<sup>15</sup> and led to values of microdomain sizes in polyurethanes in general agreement with X-ray scattering. This form is

$$D = 2r_0^2/T_{2m} \quad (7)$$

The pertinent quantities are the radius of the hydrogen atom,  $r_0$ , and the spin–spin relaxation time for the more mobile component. A second method of estimating an upper bound for  $D$  was presented by Cheung and Gerstein<sup>17</sup> and led to the form

$$D = 0.13a^2/T_{2l} \quad (8)$$

where  $a^2$  is the average square distance between adjacent protons in the less mobile domain. The intermolecular and intramolecular contributions to the second moment are roughly equivalent for the polycarbonate under study here and the principal intramolecular interaction stems from protons separated by 2.5 Å. This leads us to choose 2.5 Å as the distance to be entered into eq 8. Table III lists the  $D$ 's calculated by the two approaches represented by eq 7 and 8. The two estimates yield similar results.

With the values of  $D$ , the domain size can easily be calculated with the results shown in Table IV. The results indicate that for any dimensionality the radius of the more mobile domains is in the range 10–50 Å. Since the ratio of less mobile component to more mobile component is known from the line-shape experiments and these domains have very similar, if not the same, densities, this ratio can be assumed to be the ratio of the volumes of the two components.<sup>14–16</sup> This knowledge combined with the value of the more mobile domain size can be used to calculate a value for the less mobile domain size. The basic equation is

$$(\text{more mobile fractional population})^{1/3} = r_m/(r_l + r_m) \quad (9)$$

The symbol  $r$  is for the radius of a domain and a value of

**Table IV**  
**Domain Size**

temp, °C	$b$ , Å							
	Assink $D$				Cheung and Gerstein $D$			
	1D	2D	3D	(var lim)	1D	2D	3D	(var lim)
197	11	24	41	35	9	20	34	29
202	13	29	48	38	11	24	39	31
207	13	30	48	39	12	27	42	34

31 Å is obtained for the less mobile domain at 197 °C, given a population fraction of 0.88 for the less mobile component and a radius of 30 Å for the more mobile component.

## Discussion

Curiously enough, the first point to discuss is the fact that the GS experiment essentially works. The treatment of line shapes or FID's as consisting of only two discrete components of differing mobility is a fairly drastic and arbitrary assumption, although the appearance of the proton spectra supports the assumption. Also, a successful line-shape analysis leading to populations for the more mobile and less mobile components was carried out on the basis of this premise. This assumption underlies the selectivity of the GS experiment in the discrimination of domains. Rather than two components, it is possible that there is a continuous, *extremely* broad distribution of mobilities. Under such conditions, some types of NMR line shapes can appear bimodal<sup>4,5,12</sup> (e.g., <sup>2</sup>H NMR line shapes or any others where the inverse of the expectation value of the nuclear spin Hamiltonian is comparable or less than the time scale of the experiment). Correlation times faster than times corresponding to the regime for line-shape collapse would be lumped together as the more mobile component; sites with correlation times slower than the collapse regime would appear as the less mobile component. Thus the two components may each contain a fairly wide range of mobilities but are sufficiently distinct in terms of their respective  $T_2$ 's to provide a basis for discrimination in the GS experiment. There is also the possibility that the amorphous polymer just above the glass transition is essentially dynamically bimodal in character with two regions of rather different mobility, which appear as narrow and broad components in the line shape. If there were two such regions, at low temperature when the system is nearly rigid, rapid spin diffusion would obscure any distinguishing characteristics. As the temperature is increased, the motion increases and spin diffusion becomes less effective. At this point, the two regions would become discernible as two components in the line shape or in the FID.

In any case, the first part of the GS experiments succeeds in labeling two regions of differing mobility. The separation into two parts would indicate a dividing line of correlation times faster and slower than about 0.1 ms in the continuous distribution of correlation times model discussed above. (This is simply an order of magnitude estimate based on the line width of the spectra and the correlation time required for appreciable narrowing.) In order for the second part of the GS experiment to work, not only must a difference in mobility exist, but there must also be fairly well-defined regions associated with the differences in mobility. The two regions of differing mobility cannot be exchanged by any mechanism faster than the time scale of the mixing period. Thus either physical transport or exchange as well as spin diffusion occurs no faster than the effective inverse rate constants,  $b^2/D$ , given in Table II. In fact, we cannot distinguish between

mechanisms involving exchange of spins between the two regions by spin flips, exchange by ordinary translational diffusion, or fluctuations in free volume. No self-diffusion constants for this polymer are available, but there are self-diffusion constants available for relatively low molecular weight polystyrenes ( $9 \times 10^3$ ) at temperatures comparable to those used in these experiments.<sup>26</sup> These diffusion constants for polystyrene are of the order of  $10^{-14}$  cm<sup>2</sup>/s, which is 2 orders of magnitude slower than the spin diffusion constants given in Table III. It should also be noted that polystyrene has a glass transition temperature that is 50 deg lower than that of polycarbonate; if a temperature is considered that is only an equivalent amount above  $T_g$ , the polystyrene diffusion constant would be lowered to  $10^{-15}$  cm<sup>2</sup>/s. Furthermore, the intrinsic viscosity of the polycarbonate leads to an estimate of the molecular weight of  $2.5 \times 10^4$ . The diffusion constant for polystyrene of this molecular weight is inversely proportional to the molecular weight, whereas for the polycarbonate, which is of a molecular weight larger than the critical molecular weight, the diffusion constant should be proportional to the inverse square of molecular weight. Thus the larger molecular weight of the polycarbonate would correspond to a decrease in the diffusion constant of roughly another order of magnitude relative to the polystyrene result. Although the length scale (10–50 Å) of the GS experiment is considerably smaller than the radius of gyration of the polycarbonate, it is much larger than the mean length between entanglements ( $M_e$ ). Previous NMR studies<sup>27</sup> have shown that the macroscopic diffusion constant characterizing diffusion on the length scale of the radius of gyration is also applicable at the length scale of ( $M_e$ ). Based on these rough considerations, it would appear that the GS experiment was monitoring exchange by spin diffusion rather than translational diffusion of the polymer.

The values of the spin diffusion constants used in Table III to calculate domain size are clearly estimates. Since two different estimation procedures yield values differing by  $\sim 1.5$ , certainly the level of uncertainty in the domain sizes must be at least 25%. There is also a factor of 3 variability of the estimate of domain size on whether spin diffusion is one, two, or three dimensional in character. However, given an amorphous system with comparable intermolecular and intramolecular dipolar couplings, the three-dimensional analysis seems realistic and preferable over the lower dimensional analyses.

With the various uncertainties just listed, the domain size estimate might be expected to be correct within a factor of 3. Using the three-dimensional solution and allowing for variability of the long time limit of the value of  $R(t)$ , the best estimate for domain size at 197 °C would be 29–35 Å. The appropriate conclusion at this stage is that the domain size is in the range 10–100 Å. This in itself is an important conclusion. The domains in the amorphous polymer just above the glass transition are the size of a fraction of one polymer molecule since  $\langle R_G^2 \rangle^{1/2}$  is estimated<sup>28</sup> to be  $\sim 150$  Å for a molecular weight of  $2.5 \times 10^4$ . Thus the spatial heterogeneities in the glass, which are reflected as dynamical heterogeneities just above the glass transition temperature, involve a length scale in the range of a repeat unit to one molecule and do not involve polymolecular aggregates. Pictorially, the heterogeneities are the size of fragments of polymer molecules and many of these small heterogeneities are scattered throughout the sample. The system should not be characterized as consisting of a few large regions of mobility containing several or many polymer chains. The idea of regions of greater mobility in a glass has been discussed for phenomena below

the glass transition by Johari<sup>29</sup> in terms of islands of mobility. The results obtained here indicate that this same concept is applicable to the onset of the glass transition itself.

If one were to attempt to modify the character of the onset of mobility in an amorphous glass, such possibilities as the addition of compatible diluents or a compatible polymer might be explored to see if the domain structure were altered. In such a situation, the intermolecular interactions between a repeat unit and the immediate surroundings would be changed with the possibility of associated changes in mobility with the onset of the glass transition. The relevant interaction at the repeat unit level could be local free volume or density fluctuations or specific interactions between the polymer chain and other components of a multicomponent glass. Consideration of free volume and excess free volume have been used to characterize the population growth of the more mobile component with temperature.<sup>9–12</sup> Given the small size of the domains found here, this would appear to be the correct range of interaction to consider. Fischer et al.<sup>30</sup> have used volume fluctuations from small-angle X-ray scattering to interpret local motions below the glass transition in multicomponent polymeric glasses. The same considerations might also apply to more mobile components of glasses just above the glass transition.

The other factor that may contribute to the presence of a region of mobility just above the glass transition is a particular conformation in the polymer chain backbone. This kind of intramolecular defect has been considered as a source of the mobile regions<sup>12,31</sup> and this is again a very local source of mobility consistent with the small domains observed. The information available does not allow separation of the contributions of free volume fluctuations from the contributions of intramolecular conformations.

Although a very narrow temperature range was considered, the GS experiments indicates a growth in domain size rather than an increase in the number of domains. Over the 10 K range of this work the population of the mobile component determined from line shapes increases by one-third from 12 to 16%. Although the precision of the domain size measurement is not as good as that of the population, the domain size growth does account for all of the population change. From eq 7 to estimate  $D$  and the three-dimensional fit with variable limit, the radius of mobile domains increases from 35 to 39 Å over this temperature increment. This increase in size of the mobile domain matches the growth in the population of the narrow component of the line shape.<sup>12</sup> Because of the lack of great precision, the conclusion that the population growth appears to be by growth of domains is, at this time, tentative. If correct, this conclusion would imply that the domains would be very small at the glass transition itself and would correspond to sizes approaching a single repeat unit. This conclusion would also indicate that very local properties are the source of the onset of mobility at the glass transition.

**Acknowledgment.** This research was carried out with the financial support of the Office of Naval Research Contract N00014-87-0332 and with the financial support of E. I. du Pont de Nemours & Co.

**Registry No.** (HCO<sub>3</sub>H)(4,4'-HOC<sub>6</sub>H<sub>4</sub>C=C(Cl<sub>2</sub>)C<sub>6</sub>H<sub>4</sub>OH) (copolymer), 29057-43-0; (HCO<sub>3</sub>H)(4,4'-HOC<sub>6</sub>H<sub>4</sub>C=C(Cl<sub>2</sub>)C<sub>6</sub>H<sub>4</sub>OH) (SRU), 31546-39-1.

## References and Notes

- (1) McCall, D. W. *Acc. Chem. Res.* **1971**, *4*, 223.
- (2) Vega, A. J.; English, A. D. *Macromolecules* **1980**, *13*, 1635.

- (3) Schaefer, J.; Stejskal, E. O.; Buchdahl, R. *Macromolecules* 1977, 10, 384.
- (4) Spiess, H. W. *Colloid Polym. Sci.* 1983, 261, 193.
- (5) Spiess, H. W. *Adv. Polym. Sci.* Springer-Verlag: Berlin, 1985; Vol. 66, pp 23 ff.
- (6) Connolly, J. J.; Inglefield, P. T.; Jones, A. A. *J. Chem. Phys.* 1987, 86, 6602.
- (7) Eichhoff, U.; Zachmann, H. G. *Ber. Bunsenges. Phys. Chem.* 1970, 74, 919.
- (8) Zachmann, H. G. *Polym. Eng. Sci.* 1979, 19, 966.
- (9) English, A. D. *Macromolecules* 1984, 17, 2182.
- (10) English, A. D.; Zoller, P. *Macromolecules* 1986, 19, 2649.
- (11) English, A. D.; Zoller, P. *Anal. Chim. Acta* 1986, 189, 135.
- (12) Li, K.-L.; Inglefield, P. T.; Jones, A. A.; Bendler, J. T.; English, A. D. *Macromolecules* 1988, 21, 2940.
- (13) Goldman, M.; Shen, L. *Phys. Rev.* 1966, 144, 321.
- (14) Assink, R. A. *J. Polym. Sci., Polym. Phys. Ed.* 1977, 15, 59.
- (15) Assink, R. A. *Macromolecules* 1978, 11, 1233.
- (16) Assink, R. A.; Wilkes, G. L. *Polym. Eng. Sci.* 1977, 17, 606.
- (17) Cheung, T. T. P.; Gerstein, B. C. *J. Appl. Phys.* 1981, 52, 5517.
- (18) Packer, K. J.; Pope, J. M.; Yeung, R. R.; Cudby, M. E. A. *J. Polym. Sci., Polym. Phys. Ed.* 1984, 22, 589.
- (19) Booth, A. D.; Packer, K. J. *Mol. Phys.* 1987, 62, 811.
- (20) Havens, J. R.; Vanderhart, D. L. *Macromolecules* 1985, 18, 1663.
- (21) Cheung, T. T. P.; Gerstein, B. C.; Ryan, L. M.; Taylor, R. E.; Dybowski, C. R. *J. Chem. Phys.* 1980, 73, 6059.
- (22) Inglefield, P. T.; Jones, A. A.; Lubinez, R. P.; O'Gara, J. F. *Macromolecules* 1981, 14, 288.
- (23) Jones, A. A.; O'Gara, J. F.; Inglefield, P. T.; Bendler, J. T.; Yee, A. F.; Ngai, K. L. *Macromolecules* 1983, 16, 658.
- (24) Valeur, B.; Jarry, J. P.; Geny, F.; Monnerie, L. *J. Polym. Sci., Polym. Phys. Ed.* 1975, 13, 667.
- (25) Kambour, R. P.; Kelley, J. M.; McKinley, B. J.; Cauley, B. J.; Inglefield, P. T.; Jones, A. A. *Macromolecules* 1988, 21, 2937.
- (26) Green, P. F.; Doyle, B. L. *Macromolecules* 1987, 20, 2471.
- (27) Cohen-Addad, J. P.; Dupeyre, R. *Polymer* 1983, 24, 400.
- (28) Schnell, H. *Chemistry and Physics of Polycarbonates*; Interscience: New York, 1964; p 123.
- (29) Johari, G. P. *J. Physique Colloq.* 1985, C8, 567.
- (30) Fischer, E. W.; Hellmann, G. P.; Spiess, H. W.; Horth, F. J.; Ecarius, U.; Wehrle, M. *Makromol. Chem. Suppl.* 1985, 12, 189.
- (31) Bendler, J. T.; Shlesinger, M. F. *J. Mol. Liq.* 1987, 36, 37.

## Studies on Alternating Radical Copolymerization. Analysis of Microstructures of Styrene-Maleic Anhydride, Styrene-Acrylonitrile, and Styrene-Methyl Methacrylate Copolymers by Fluorescence Spectroscopy

Weiping Zeng and Yasuhiko Shirota\*

*Department of Applied Chemistry, Faculty of Engineering, Osaka University, Yamadaoka, Suita, Osaka 565, Japan. Received December 12, 1988;  
Revised Manuscript Received April 3, 1989*

**ABSTRACT:** Microstructures of poly(styrene-co-maleic anhydride), poly(styrene-co-acrylonitrile), and poly(styrene-co-methyl methacrylate) obtained by radical copolymerizations at various monomer feeds have been characterized by fluorescence spectroscopy. The results show that the microstructure of poly(styrene-co-maleic anhydride) varies depending on the monomer feed composition despite the fact that the overall copolymer composition is nearly 1:1; the styrene-styrene diad fraction increases with an increase in the styrene mole fraction in the monomer feed. Poly(styrene-co-acrylonitrile) obtained by spontaneously initiated radical copolymerization in the presence of zinc chloride is shown to be a real 1:1 alternating copolymer. Poly(styrene-co-methyl methacrylate) obtained in a similar manner deviates significantly from 1:1 composition. The present study shows that fluorescence spectroscopy is a useful and sensitive method for gaining information on the microstructure of copolymers formed from aryl vinyl monomers.

### Introduction

There have been extensive studies on alternating radical copolymerizations from both synthetic and mechanistic interests.<sup>1-3</sup> The styrene (St)-maleic anhydride (MAN) system has long been regarded as a 1:1 alternating radical copolymerization system and studied most intensively.<sup>4-16</sup> The mechanism for the alternating radical copolymerization of the St-MAN system has been interpreted either by the penultimate model<sup>6-8</sup> or by charge-transfer models involving the participation of monomer charge-transfer complex in the propagation;<sup>9-14</sup> however, it still remains to be clarified.

Characterizations of copolymers as 1:1 alternating copolymers have usually been done on the basis of equimolar composition over a wide range of monomer feed ratios. For example, composition data of poly(St-co-MAN) obtained by copolymerizations both in solvents and in bulk show that copolymer compositions are nearly equimolar when the mole fraction of MAN greater than 0.1.<sup>8,14-16</sup> Thus the St-MAN system has been regarded as a 1:1 alternating

copolymerization system. However, the equimolar composition of copolymers does not necessarily mean that they are truly 1:1 alternating copolymers. In addition, there is a limitation in the accuracy of copolymer compositions, which have usually been determined by elemental analysis, infrared absorption spectroscopy, or chemical analysis. It is therefore necessary to distinguish real 1:1 alternating copolymers from copolymers with a statistical 1:1 composition. This distinction requires information on the microstructure of copolymers.

In spite of extensive studies on 1:1 alternating radical copolymerizations, there have been only a few studies on the microstructure of the copolymers. The monomer sequence distribution of poly(St-co-MAN) has been studied by <sup>13</sup>C NMR spectroscopy.<sup>14,17-19</sup> It has been reported that the copolymerization with an excess mole fraction of styrene results in deviation from the alternating structure when the resonance of the aromatic carbon attached to the polymer chain is considered.<sup>18</sup> On the contrary, more recent results based on the <sup>13</sup>C NMR methylene resonance